

Unusual Carbonyl···Carbonyl Interaction in Supramolecular Structures of Silver(I) Complexes with 2,6-Pyridinediylbis(4-pyridinyl)methanone

Chong-Qing Wan^{†,‡} and Thomas C. W. Mak^{*,†}[†]Department of Chemistry and Center of Novel Functional Molecules, The Chinese University of Hong Kong, Shatin, New Territories, Hong Kong SAR, P. R. China, and [‡]Department of Chemistry, Capital Normal University, Beijing 100048, P. R. China

Received November 9, 2010; Revised Manuscript Received January 4, 2011

ABSTRACT: A series of silver(I) complexes of a higher homologue of di-2-pyridyl ketone, 2,6-pyridinediylbis(4-pyridinyl)methanone (abbreviated as L), consisting of {[Ag(L)(BF₄)·H₂O]}_∞ (**1**), {[Ag(L)(NO₃)·H₂O]}_∞ (**2**), [Ag₃(L)₂(NO₂)₃(H₂O)]_∞ (**3**), [Ag(L)₂(PF₆)₂] (**4**), {[Ag(L)(CO₂CF₃)₂]}_∞ (**5**), [Ag(L)₂(SO₃CF₃)₂] (**6**), and [Ag(L)₂(CO₂CF₂CF₃)₂] (**7**), have been synthesized and characterized. Complexes **1** and **2** are isomorphous helical polymers, **3** is a metallacycle featuring a trisilver(I) core, and **4–7** are isostructural complexes containing a common dinuclear [Ag₂(L)₂]²⁺ metallacyclic skeleton. All complexes except **4** feature a common dominant intermolecular multipolar carbonyl···carbonyl interaction, which along with argentophilic Ag(I)···Ag(I), π···π, hydrogen-bonding, Ag···O=C, O(trifluoroacetate)···C=O as well as unconventional C=O···π and anion-π(pyridyl) interactions assemble the different coordination motifs (**1–3**, **5–7**) into higher-dimensional frameworks. Three principal types of carbonyl···carbonyl interaction exhibiting antiparallel, sheared parallel, and perpendicular motifs are observed, and unusual supramolecular associations such as “···[C=O···C=O]_n···” (in **1–2** and **6**) and “···[C=O···C=O···π]_n···” (in **3**) and “C=O···C=O···C=O” (in **7**) are the novel structural features established in these complexes. The geometrical parameters and role of such noncovalent interactions in the construction of the present series of supramolecular metal–organic frameworks are discussed.

Introduction

The carbonyl group, owing to its ubiquitous occurrence in organic and biological systems, plays a crucial role in stabilizing protein secondary structure motifs and molecular recognition processes through intermolecular carbonyl···carbonyl interaction.¹ In recent years, a growing body of literature typified by the work of Gavezzotti,² Allen,³ Lee,⁴ and others⁵ focuses on the presence, geometry, and strength of this type of noncovalent interaction via crystal structure analyses, computational studies, and database searches in the Cambridge Structural Database (CSD) and Protein Data Bank (PDB).⁶ It is now well recognized that such weak dipolar···dipolar (C=O^(δ-)···C^(δ+)=O) contact widely exists in small molecules and protein–ligand complexes, and electrostatic factors are important in determining its total interaction energies and geometry.^{4,7} Diederich and co-workers also concluded that the intermolecular carbonyl···carbonyl interaction with orthogonal motif is potentially important for both structural chemistry and biological molecular recognition.⁸ However, further endeavor is required for a systematic study on the role of carbonyl···carbonyl interaction in stabilizing both the extended crystal structures of small molecules and biological systems, especially in the construction of supramolecular metal–organic hybrid frameworks.⁹

In order to conduct a systematic investigation on the role of intermolecular carbonyl···carbonyl interaction in the conglomeration of crystalline metal–organic complexes, we have designed and synthesized the oligo-pyridyl ketone ligand 2,6-pyridinediylbis(4-pyridinyl)methanone (abbreviated as L, Scheme 1). The carbonyl groups of this multidentate ligand

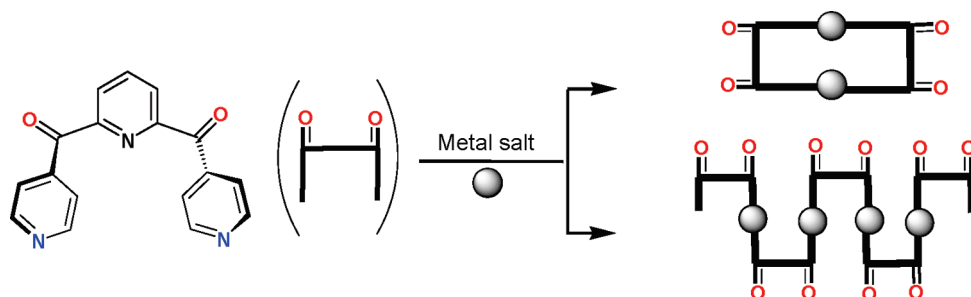
are expected to provide possible intermolecular carbonyl···carbonyl interaction in supramolecular conglomeration of its metal complexes. In the present context, we report seven silver(I) complexes derived from L and silver(I) salts, namely, {[Ag(L)(BF₄)·H₂O]}_∞ (**1**), {[Ag(L)(NO₃)·H₂O]}_∞ (**2**), [Ag₃(L)₂(NO₂)₃(H₂O)]_∞ (**3**), [Ag(L)₂(PF₆)₂] (**4**), {[Ag(L)(CO₂CF₃)₂]}_∞ (**5**), [Ag(L)₂(SO₃CF₃)₂] (**6**), and [Ag(L)₂(CO₂CF₂CF₃)₂] (**7**), which were characterized through elemental analysis, FT-IR spectroscopy, and X-ray crystallography.

Experimental Section

General. Diethyl ether was purchased from LAB-SCAN and further refluxed over sodium and benzophenone. All other organic reagents were purchased from Aldrich and used without further purification. The silver(I) salts were obtained from commercial sources. The L ligand readily reacted with various silver(I) salts, and crystallization by slow evaporation of the solvent yielded a series of silver(I) complexes **1–7**. Changing the reaction ratio between L and the Ag(I) salt did not affect the synthesis, and the same product was obtained in each case. Elemental analyses of C, H, and N were performed by the MEDAC LTD Brunel Science Centre, United Kingdom. IR spectra were recorded with a Nicolet Impact 420 FT-IR spectrometer using KBr pellets. ¹H NMR spectra were taken with a 300 MHz Bruker-300 spectrometer.

Synthesis of 2,6-Pyridinediylbis(4-pyridinyl)methanone (L). The ligand synthesis was performed under a nitrogen atmosphere using standard Schlenk techniques. 4-Bromopyridine hydrochloride (1.96 g, 10 mmol) was added to a 40 mL methanolic solution of KOH (0.56 g, 10 mmol) with vigorous stirring for half an hour. MgSO₄ (5 g) was added, and the solution was then left to stand at room temperature for 1 h. After filtration, the colorless solution was concentrated in vacuo to give a yellow oil of 4-bromopyridine which was then dissolved in 40 mL of anhydrous diethyl ether and cooled to -90 °C for further reaction. *n*-Butyllithium (1.6 M in hexane, 7 mL, 11 mmol) in 20 mL of anhydrous diethyl ether was slowly added to the 4-bromopyridine solution with stirring at -90 °C for 30 min.

*Author for correspondence. Tel.: +852-2609 6279; fax: +852-2603 5057; e-mail: tcwmak@cuhk.edu.hk.

Scheme 1. Schematic Illustration of Coordination Motifs Bearing Multiple Carbonyl Groups Constructed with the Multidentate Ligand 2,6-Pyridinediylbis(4-pyridinyl)methanone**Table 1. Crystallography Data for Complexes 1–7**

	1	2	3	4	5	6	7
empirical formula	C ₁₇ H ₁₃ BF ₄ N ₃ O ₃ Ag	C ₁₇ H ₁₃ N ₄ O ₆ Ag	C ₃₄ H ₂₄ N ₉ O ₁₁ Ag ₃	C ₃₄ H ₂₂ N ₆ O ₄ F ₁₂ P ₂ Ag ₂	C ₁₉ H ₁₁ N ₃ O ₄ F ₃ Ag	C ₃₆ H ₂₂ N ₆ O ₁₀ F ₆ S ₂ Ag ₂	C ₂₀ H ₁₁ F ₅ N ₃ O ₄ Ag
formula weight	501.97	477.17	1058.23	1084.26	510.18	1092.46	560.19
<i>T</i> /K	293(2)	293(2)	293(2)	293(2)	293(2)	293(2)	293(2)
crystal system	monoclinic	monoclinic	monoclinic	triclinic	triclinic	monoclinic	triclinic
space group	<i>P</i> 2 ₁ / <i>c</i>	<i>P</i> 2 ₁ / <i>c</i>	<i>P</i> 2 ₁	<i>P</i> $\bar{1}$	<i>P</i> $\bar{1}$	<i>C</i> 2/ <i>c</i>	<i>P</i> $\bar{1}$
crystal size/mm ³	0.43 × 0.37 × 0.27	0.33 × 0.22 × 0.19	0.45 × 0.32 × 0.29	0.31 × 0.21 × 0.19	0.38 × 0.20 × 0.12	0.42 × 0.32 × 0.29	0.45 × 0.32 × 0.26
$\Delta\rho_{\max}/\Delta\rho_{\min}$ (e Å ⁻³)	0.723/−0.590	0.76/−0.362	0.643/−1.002	1.439/−1.252	0.935/−0.495	1.050/−0.556	0.844/−0.511
<i>a</i> /Å	13.366(2)	13.469(2)	6.875(2)	6.838(2)	8.297(1)	30.277(5)	9.399(4)
<i>b</i> /Å	10.790(2)	10.614(2)	10.444(2)	10.435(3)	8.474(1)	7.062(1)	9.791(5)
<i>c</i> /Å	12.769(2)	12.643(2)	25.018(5)	13.230(4)	13.966(2)	20.801(4)	12.087(6)
α /°	90	90	90	96.019(5)	100.676(3)	90	93.867(9)
β /°	93.432(4)	92.801(5)	91.677(4)	104.732(6)	94.563(3)	117.585(3)	102.894(8)
γ /°	90	90	90	94.695(6)	104.608(3)	90	108.332(9)
<i>V</i> /Å ³	18382(6)	1805.4(5)	1795.5(6)	902.1(4)	925.5(2)	3941.9(1)	1017.8(8)
<i>Z</i>	4	4	2	1	2	4	2
<i>D</i> _c /g cm ⁻³	1.807	1.748	1.957	1.996	1.831	1.841	1.828
θ /°	1.53–28.32	1.51–28.31	0.81–28.28	1.98–23.28	1.50–25.00	1.52–25.01	2.22–25.01
<i>F</i> (000)	984	944	1040	532	504	2160	552
μ (Mo–K α)/mm ⁻¹	1.160	1.160	1.695	1.287	1.152	1.194	1.070
reflections collected	12555	12990	12525	4240	5071	10256	5549
independent reflections (<i>R</i> _{int})	4538 (0.0245)	4462 (0.0378)	8468 (0.0260)	2592 (0.0425)	3246 (0.0243)	3465 (0.0262)	3570 (0.0187)
observed reflections [<i>I</i> > 2 σ (<i>I</i>)]	3174	2502	6286	1886	2724	2879	3070
parameters	261	271	541	275	271	281	298
goodness-of-fit (<i>F</i> ²)	1.038	1.005	1.075	1.044	1.036	1.031	1.090
<i>R</i> ₁ [<i>I</i> > 2 σ (<i>I</i>)] ^a	0.0537	0.0469	0.0434	0.0691	0.0450	0.0386	0.0456
<i>wR</i> ₂ (all data) ^b	0.1776	0.1528	0.0964	0.1923	0.1283	0.1108	0.1318

$$^a R_1 = \sum |F_o| - |F_c| / \sum |F_o|, \quad ^b wR_2 = \{\sum [w(F_o^2 - F_c^2)^2] / \sum [w(F_o^2)^2]\}^{1/2}.$$

Subsequently, dimethyl 2,6-pyridinedicarboxylate (0.975 g, 5 mmol) dissolved in a mixed solvent of 8 mL of anhydrous diethyl ether, and 2 mL of tetrahydrofuran was added dropwise with vigorous stirring within 30 min. After being stirred at −90 °C for another 30 min, the solution was slowly warmed to room temperature and allowed to stand overnight, after which it was further quenched with 50 mL HCl solution in water and methanol (water/methanol/conc HCl = 5:5:1) at −40 °C. The crude product was extracted with chloroform, and the combined organic extract was dried over anhydrous magnesium sulfate and finally concentrated in vacuo to give a brown oil. Further purification by chromatography on silica gel using ether acetate/dichloromethane/methanol (3:9:1) as the eluent gave 0.38 g of colorless powdery 2,6-pyridinediylbis(4-pyridinyl)methanone (L) in 26% yield; mp 115–119 °C; ¹H NMR (300 MHz, CDCl₃): δ 8.73(dd, 4H), 8.45 (d, 2H), 8.22 (t, 1H), 7.83 (dd, 4H); IR (KBr): 1669 cm⁻¹ (C=O). Elem. Anal. Calcd (Found) for C₁₇H₁₁N₃O₂: C, 70.58 (70.22); H, 3.83 (3.54); N, 14.52 (14.77) %.

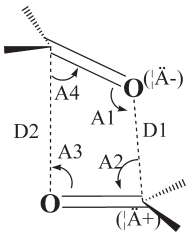
Synthesis of {[Ag(L)](BF₄)·H₂O}_∞ (1). Reaction of 2,6-pyridinediylbis(4-pyridinyl)methanone (L; 30 mg, 0.1 mmol) and AgBF₄ (19.5 mg, 0.1 mmol) in a mixed solvent of 2 mL of

acetonitrile and 1 mL of methanol gave a white precipitate, which was dissolved by adding 1 mL of deionized water. The yield solution was stirred at room temperature for 2 h. After filtration, the clear solution was then left to stand in air for five days. Yellow block-like crystals of **1** were deposited. Yield: 49.50 mg (75%). Elem. Anal. Calcd. (Found) for C₁₇H₁₃N₃O₃BF₄Ag: C, 40.68 (40.75); H, 2.61 (2.45); N, 8.37 (8.58) %. IR (KBr) ν /cm⁻¹: 3435(m), 1669(vs), 1555(w), 1394 (vs), 1313(vs), 1246(w), 1071(m), 1023(m), 937(w), 850(w), 749(w), 648(m).

Synthesis of {[Ag(L)](NO₃)·H₂O}_∞ (2). Ligand L (30 mg, 0.1 mmol) and AgNO₃ (17 mg, 0.1 mmol) were dissolved in a mixed solvent of 2 mL of acetonitrile and 1 mL of methanol with stirring at room temperature for 2 h to yield a clear yellow solution. After filtration, the solution was then left to stand in air for four days to afford colorless crystals of **2**. Yield: 39.11 mg (80%). Elem. Anal. Calcd. (Found) for C₁₇H₁₃N₄O₆Ag: C, 42.86 (42.81); H, 2.75 (2.58); N, 11.74 (11.53) %. IR (KBr) ν /cm⁻¹: 3435(w), 1669(m), 1548(w), 1387(vs), 1320(m), 1226(w), 1158(w), 1078(w), 937(w), 850(w), 742(w), 640(w).

Synthesis of [Ag₃(L)₂(NO₂)₃(H₂O)_∞ (3). Yellow block-like crystals of **3** were obtained in a similar manner as in the synthesis of **1**.

Table 2. The Geometries and Metric Parameters of Intermolecular Carbonyl...Carbonyl Interactions in Complexes 1–7



complex	A1 (deg)	A2 (deg)	A3 (deg)	A4 (deg)	D1 (Å)	D2 (Å)	torsion angle τ (deg)	C=O...C=O configuration
1	118.2	98.5	72.8	57.0	3.121	4.025	57.0	antiparallel
	121.5	92.7	63.4	37.2	3.216	4.381	122.9	sheared parallel
2	120.4	99.9	71.1	54.8	3.121	4.104	58.6	antiparallel
	122.5	93.4	63.2	36.8	3.278	4.471	123.1	sheared parallel
3	87.1	99.7	79.4	91.5	3.319	3.489	19.7	antiparallel
4								
5	125.6	102.6	57.2	37.5	2.975	4.335	110.4	sheared parallel
6	161.3	104.0	63.5	22.5	3.315	4.887	72.1	perpendicular
7	90	90	90	90	3.194	3.194	0	antiparallel
	88.0	65.5	84.7	62.3	3.432	3.505	117.8	sheared parallel

Yield: 35.00 mg (67%). Elem. Anal. Calcd. (Found) for $C_{34}H_{24}N_9O_{11}Ag_3$: C, 38.52 (38.80); H, 2.29 (2.19); N, 11.91 (11.63)%. IR (KBr) ν/cm^{-1} : 3423(w), 1666(vs), 1540(w), 1412(m), 1315(m), 1262(vs), 1061(w), 992(m), 940(m), 857(w), 745(m), 662(w).

Synthesis of $[Ag(L)]_2(PF_6)_2$ (4). Colorless crystals of complex 4 were obtained following the procedure used for 2. Yield: 33.72 mg (62%). Elem. Anal. Calcd. (Found) for $C_{17}H_{11}N_3O_2PF_6Ag$: C, 37.66 (37.75); H, 2.05 (2.30); N, 7.75 (7.88)%. IR (KBr) ν/cm^{-1} : 3423(w), 1698(vs), 1608(w), 1555(w), 1435(vs), 1330(vs), 1255(w), 1180(w), 1075(w), 993(w), 843(vs), 693(w), 655(m), 558(s).

Synthesis of $\{[Ag(L)(CO_2CF_3)]_2\}_\infty$ (5). Ligand L (30 mg, 0.1 mmol) and $AgCO_2CF_3$ (22 mg, 0.1 mmol) were dissolved in a mixed solvent of 2 mL of acetonitrile and 1 mL of methanol. A yellow precipitate was afforded subsequently. The cloudy mixture changed to a clear yellow solution upon addition of another 2 mL of acetonitrile. Colorless crystals of 5 suitable for X-ray crystallographic analysis were deposited after four days. Yield: 36.10 mg (70%). Elem. Anal. Calcd. (Found) for $C_{19}H_{11}N_3O_4F_3Ag$: C, 44.73 (44.78); H, 2.17 (2.18); N, 8.24 (8.54)%. IR (KBr) ν/cm^{-1} : 3402(m), 1682(vs), 1407(m), 1320(m), 1212(vs), 1118(s), 894(w), 930(w), 829(m), 735(w), 648(m).

Synthesis of $[Ag(L)]_2(SO_3CF_3)_2$ (6). Colorless complex 6 was obtained in a similar manner as in the preparation of 2. Yield: 44.01 mg (70%). Elem. Anal. Calcd. (Found) for $C_{18}H_{11}N_3O_5F_3SAg$: C, 39.58 (39.45); H, 2.03 (2.00); N, 7.69 (7.66)%. IR (KBr) ν/cm^{-1} : 3429(w), 1702(m), 1669(s), 1548(w), 1420(w), 1279(vs), 1158(s), 1038(m), 977(w), 937(w), 856(w), 749(w), 648(m), 527(w).

Synthesis of $[Ag(L)]_2(CO_2CF_2CF_3)_2$ (7). This complex was afforded following the procedure used for 4. Yield: 46.00 mg (82%). Elem. Anal. Calcd. (Found) for $C_{20}H_{11}N_3O_4F_5Ag$: C, 42.88 (42.55); H, 1.98 (1.99); N, 7.50 (7.55)%. IR (KBr) ν/cm^{-1} : 3429(w), 1669(vs), 1555(w), 1421(m), 1347(vs), 1226(vs), 1159(vs), 1023(m), 944(w), 857(w), 837(m), 743(m), 662(w), 649(w).

X-ray Data Collection and Structure Refinement. Single-crystal X-ray diffraction data of complexes 1–7 were collected on a Bruker Smart 1000 CCD diffractometer operating at 50 kV and 30 mA using MoK α radiation ($\lambda = 0.71073$ Å) at 293 K. Data reduction was performed using the SMART and SAINT software.¹⁰ An empirical absorption correction was applied using the SADABS program.¹¹ All structures were solved by direct methods and refined by full-matrix least-squares on F^2 using the SHELXTL program package.¹² The ordered non-hydrogen atoms in each structure were refined with anisotropic thermal parameters, while the H atoms were placed in idealized positions and allowed to ride on their respective parent carbon atoms. The crystallographic data and refinement parameters of 1–7 are summarized in Table 1. In complex 1–2, the lattice water O1w is disordered over two sites of equal occupancy, and their hydrogen atoms were omitted in the refinement. The disordered F3 atom of 1 occupies two half-populated sites. In 2, O5 is disordered over two

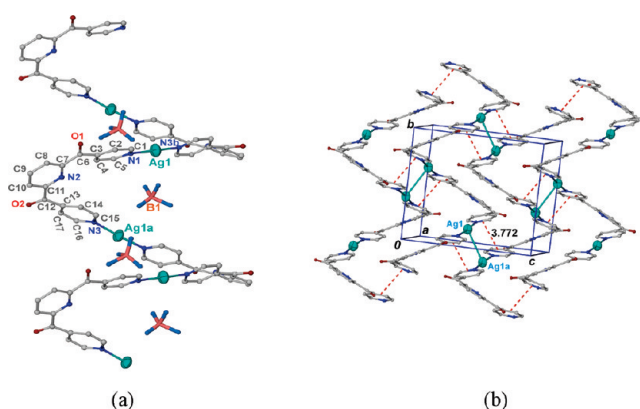


Figure 1. (a) Helical structure of 1. Symmetry codes: a: $-x + 2, y - 1/2, -z + 3/2$; b: $-x + 2, y + 1/2, -z + 3/2$. (b) Argentophilic (turquoise bonds) and $\pi \cdots \pi$ stacking (red dashed lines) interactions between the 2₁ helices of opposite chirality lying approximately parallel to the bc plane. Symmetry code: a $-x - 2, -y, -z + 2$.

positions in a ratio of 3:2. In 3, the N7 and N8 atoms are each 2-fold disordered.

Results and Discussion

To facilitate subsequent discussion, we define the geometrical parameters of the carbonyl...carbonyl interaction as follows: the torsion angle of $C=O^{(\delta-)} \cdots C^{(\delta+)}=O$ is designated as τ (see Table 2), which takes the value zero for the planar antiparallel arrangement of two C=O groups; A1–A4 represent $C=O^{(\delta-)} \cdots C^{(\delta+)}$, $O^{(\delta-)} \cdots C^{(\delta+)}=O$, $C^{(\delta+)}=O \cdots C$, and $O \cdots C=O^{(\delta-)}$, respectively; D1 represents the $O^{(\delta-)} \cdots C^{(\delta+)}$ distance, while D2 indicates the $O \cdots C$ separation. In the present context, the measured values of D1 lie within the 2.975–3.432 Å range, being close to the sum of van der Waals radii (3.12 Å) of the interacting atoms based on the Pauling's scale¹³ plus 0.2 Å as a standard reference. The values of D1 and D2 are given three digits after the decimal point, while all that of angles (A and τ) are given one digit. The detailed geometrical parameters of C=O...C=O interactions revealed in supramolecular conglomeration of complexes 1–7 are summarized and compared in Table 2.

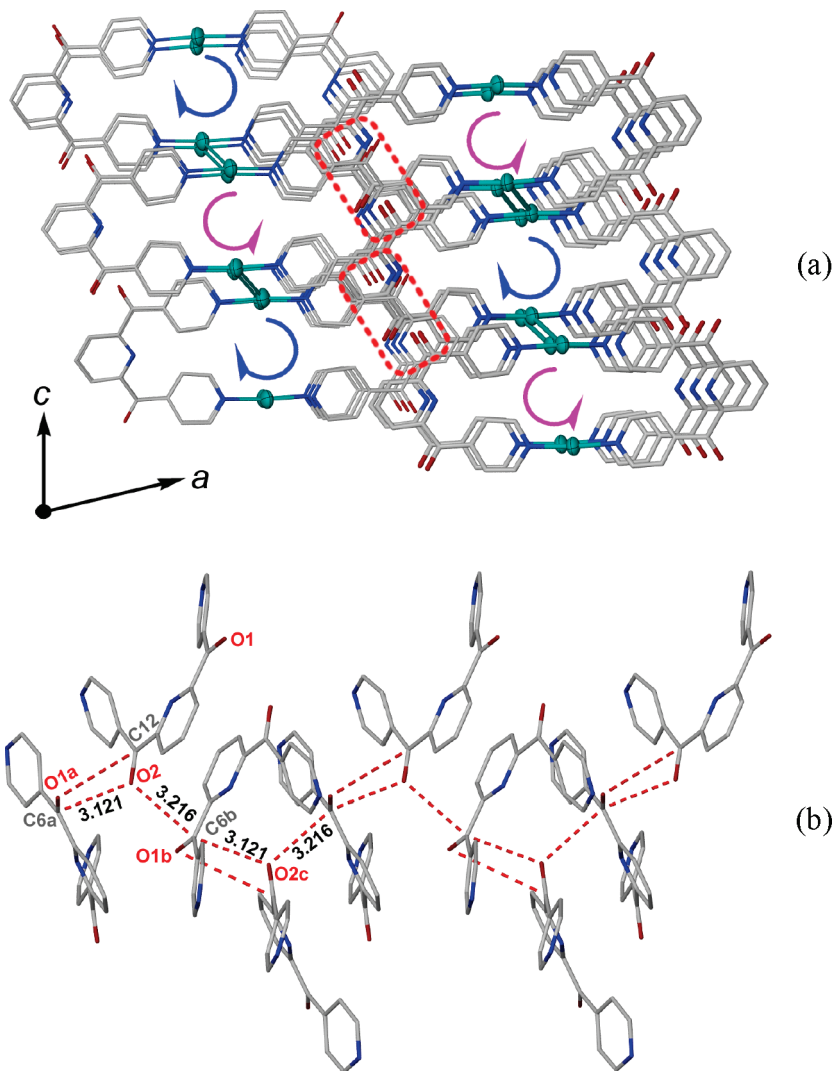


Figure 2. (a) Molecular packing in **1** viewed down the b axis. The arrows with different colors indicate right- and left-handed helices, and the turquoise bonds represent argentophilic interactions. The encircled portions indicate the sites of the carbonyl \cdots carbonyl contact between the helices. All hydrogen atoms and anions as well as $\pi\cdots\pi$ interactions are omitted for clarity. (b) An $\cdots[\text{C}=\text{O}\cdots\text{C}=\text{O}]_n\cdots$ array with the carbonyl \cdots carbonyl interactions within an encircled portions on part (a). Symmetry codes: a: $x, -y + 1/2, z - 1/2$; b: $-x + 1, -y + 1, -z + 1$; c: $-x + 1, y + 1/2, -z + 1/2$.

Complexes **1** and **2** are isomorphous helical polymers despite the fact that their respective anionic components BF_4^- (**1**) and NO_3^- (**2**) are significantly different in volume and geometry. The low unit-cell similarity index of 0.005 between them indicates that they are nearly isostructural, and a parallel description of their crystal structures will be conducted. Complex **3** is a metallacycle featuring a trisilver(I) core, while **4–7** comprise a series of isostructural complexes containing a common disilver(I) $[\text{Ag}_2(\text{L})_2]^{2+}$ metallacycle, which will be separately discussed. In these complexes, the L ligand can be viewed as two pendant 4-pyridyl rings attached to a central pyridyl skeleton via separate carbonyl bridges, acting in the μ_2 -bridging mode with its 4-pyridyl N atoms bound to separate Ag(I) ions.

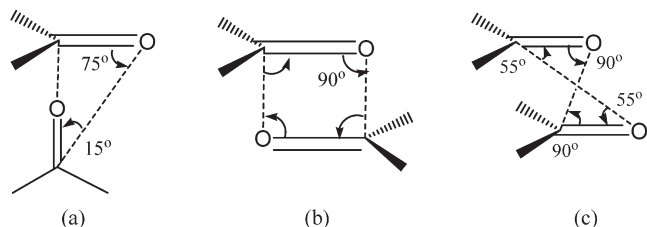
For isomorphous complexes $\{[\text{Ag}(\text{L})](\text{BF}_4)\cdot\text{H}_2\text{O}\}_\infty$ (**1**) and $\{[\text{Ag}(\text{L})](\text{NO}_3)\cdot\text{H}_2\text{O}\}_\infty$ (**2**), each Ag(I) adopts approximately linear coordination (N1–Ag1–N3b 175.81(1) $^\circ$ in **1**; N1–Ag1–N3b 176.79(1) $^\circ$ in **2**; b $-x + 2, y + 1/2, -z + 3/2$) with two L ligands around it (Figure 1a), while each μ_2 -bridging L links two Ag(I) ions with the C3–C6 \cdots C12–C13 torsion angle of 18.6 $^\circ$ in **1** and 16.9 $^\circ$ in **2**, generating a 2_1 helical

moiety along the b axis with counteranions embedded within the crystal lattice of each complex. Helices of opposite chirality alternatively arranged along the c direction are interconnected through argentophilic (Ag \cdots Ag 3.560(4) Å in **1**, 3.575(4) Å in **2**)¹⁴ and $\pi\cdots\pi$ interactions between 4-pyridyl rings (centroid \cdots centroid 3.772 Å in **1**, 3.788 Å in **2**) to form a layer in the bc plane, as shown in Figure 1b. The layers stack along the a axis with the protruding 2,6-pyridinediyl rings of adjacent layers interdigitating and stacking at a centroid \cdots centroid distance of 4.134 Å in **1** and 4.185 Å in **2**, respectively. Interesting intermolecular carbonyl \cdots carbonyl interactions occur between the carbonyl groups from adjacent layers, which combine with $\pi\cdots\pi$ interactions between the 2,6-pyridinediyl rings to link the layers together, forming a three-dimensional framework (Figure 2a).

Regarding the carbonyl \cdots carbonyl interaction of **1**, as shown in Figure 2b, one carbonyl group (C12=O2) is in contact with two others (C6a = O1a, C6b = O1b, a: $x, -y + 1/2, z - 1/2$; b: $-x + 1, -y + 1, -z + 1$), stacking along the b axis with the closest O $^{(\delta-)}\cdots$ C $^{(\delta+)}$ contact at 3.121 and 3.216 Å (D1), respectively, thereby generating a $\cdots[\text{C}=\text{O}\cdots\text{C}=\text{O}]_n\cdots$ array.

These values are close to the sum of van der Waals radii (3.12 Å) of the interacting atoms based on Pauling's scale,¹³ being comparable with the range 2.92–3.32 Å from computational studies on a bis-propanone dimer model.^{3a} For the C12=O2···C6a = O1a contact, the A1 and A2 values are 118.2° and 98.5°, respectively, and the τ angle equals 57.0°, which are comparable to the statistically averaged geometry of the antiparallel motif (A1 = 96.5°, A2 = 83.5°, $\tau \leq 20^\circ$)

Scheme 2. Three Types of Idealized Intermolecular Carbonyl···Carbonyl Interactions: (a) Perpendicular Motif; (b) Anti-Parallel Motif; (c) Sheared Parallel Motif



based on CSD research by Allen.^{3a} Accordingly, we assign this interaction geometry as belonging to the antiparallel motif (Scheme 2). For the C12=O2···C6b=O1b interaction, the values of A1–A4 vary from 37.2° to 121.5°, while τ is 122.9°, and thus we designate this case as the sheared parallel motif (Scheme 2). The detailed metric parameters of these interactions are listed in Table 2. Since the structure of **2** is similar to that of **1**, the corresponding numerical values of angles A1 to A4 and C···O distances D1 and D2 are listed in Table 2 for comparison.

Complex [Ag₃(L)₂(NO₂)₃(H₂O)]_∞ (**3**) is a metallacyclophane featuring a trisilver(I) core with three independent silver(I) ions in the asymmetric unit (Figure 3a). The Ag1 atom adopts a trigonal N₂O-coordination geometry surrounded by 4-pyridyl N atoms of two L ligands and one monodentate nitrite (N9 containing) O atom, and it furthermore weakly interacts with O5 (N7 containing nitrite) at 2.875(6) Å. The Ag2 atom exhibits tetrahedral N₃O-coordination geometry with two 4-pyridyl N atoms, one aqua ligand, and one nitrite N atom (N8 containing) around it. The third

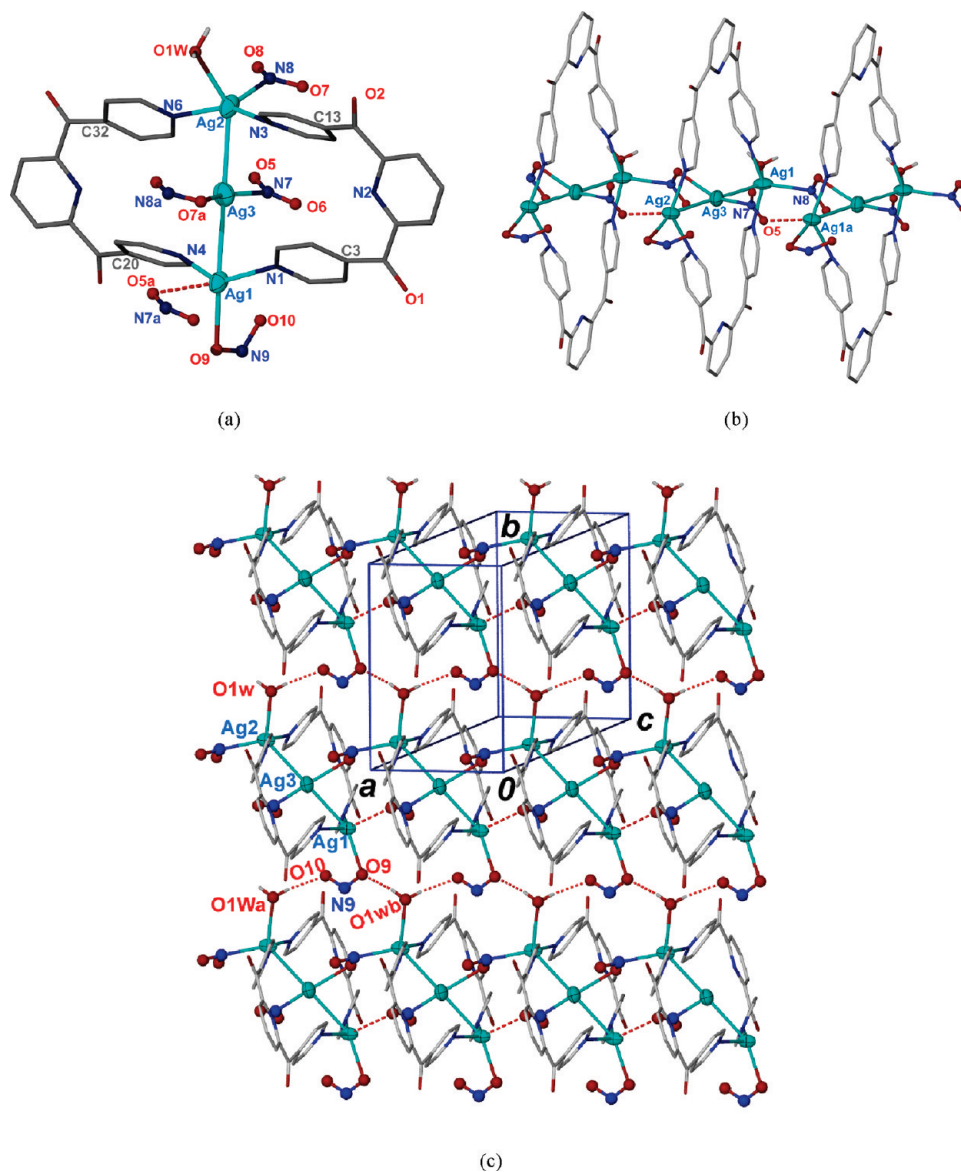


Figure 3. (a) Coordination geometries of Ag(I) in **3**. Symmetry code: a: $x + 1, y, z$. (b) Infinite trisilver(I) chain linked by nitrite and Ag···O interaction. Symmetry code: a: $x - 1, y, z$. (c) Hydrogen-bonding linkage between trisilver(I) chains. Symmetry codes: a: $x, y - 1, z$; b: $x + 1, y - 1, z$.

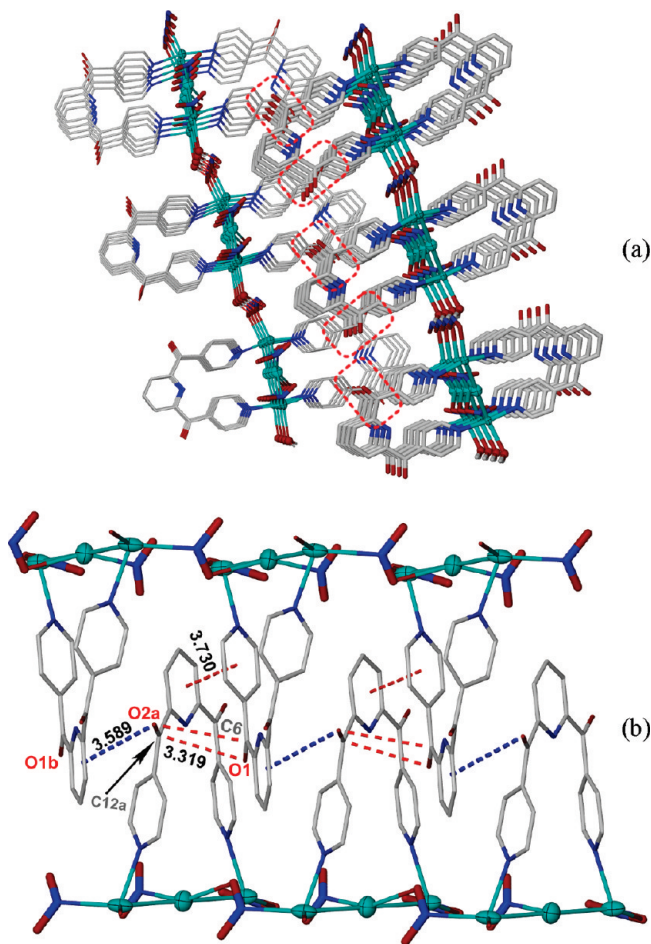


Figure 4. (a) Molecular packing viewed along the *a* axis in the 3-D framework of **3**. The encircled portion indicates the existence of carbonyl...carbonyl interactions. All hydrogen atoms except for that of water molecules are omitted for clarity. (b) Molecular packing provided by C=O... π (blue dashed lines), π ... π , and carbonyl...carbonyl interactions (red dashed lines), corresponding to the encircled portions in (a) part. Symmetry codes: a: $-x + 1, y - 1/2, -z + 1$; b: $x + 1, y, z$.

Ag3 atom has an approximate linear coordination with two independent nitrite ligands bonding at their N (N7 containing) and O atoms (N8 containing), respectively. As shown in Figure 3a, a pair of L ligands bridges Ag1 and Ag2 atoms through four 4-pyridyl N atoms to form a metallacycle, while Ag3 is located between Ag1 and Ag2 and in contact with both atoms through argentophilic interactions (3.014(1) Å, 3.043(1) Å). Because of the huddling Ag3 atoms within the metallacycle, Ag1 and Ag2 are pushed outward with N1–Ag1–N4 and N3–Ag2–N6 angles of 135.5(2)° and 149.15(2)°, respectively, being much smaller than values of about 176° found in the linearly coordinated Ag(I) ions of **1** and **2**.

The silver(I) metallacycles are bridged by the $\mu_{(N,O)}$ -nitrite ligand (N8 containing) and Ag1a...O5 (N7 containing nitrite) interaction to form an infinite chain along the *a* direction, as shown in Figure 3b. The chains are further interconnected through hydrogen bonding of bridging O1W to generate a layer in the *ab* plane (O1Wa–H1WA...O10 169°, O1Wa...O10 2.905(8) Å, O1 Wb–H1W...O9 173°, O1 Wb...O9 2.737(8) Å) (Figure 3c). The parallel chains along the *a* direction with the metallacyclic [Ag₃(L)₂]³⁺ motifs interdigitate and stack with the L moieties. Intermolecular carbonyl...carbonyl interactions occur between pairs of

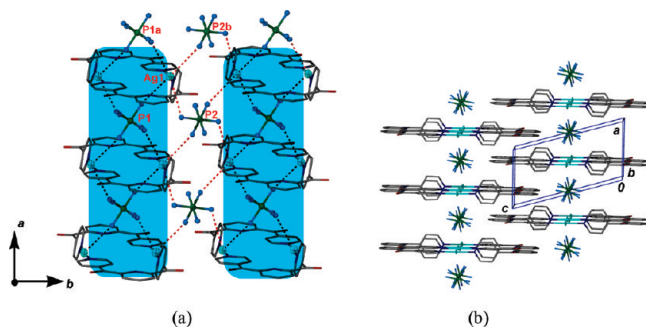


Figure 5. (a) Ag...F(PF₆⁻) interactions in **4**. The highlighted portions indicate the stacked columns in **4**. Symmetry codes: a: $-x + 1, -y + 1, -z + 1$; b: $-x + 1, -y + 2, -z + 1$. (b) Lateral view of the stacking of metallacycles. All hydrogen atoms and noncovalent interactions are omitted for clarity.

overlapping carbonyl groups, which combine with the coexisting C=O... π (pyridyl) contact and π ... π interaction (centroid...centroid 3.730 Å) between the 4-pyridyl and 2,6-pyridinediyl rings to link the chains together, generating a 3-D supramolecular framework (Figure 4a). As shown in Figure 4b, a pair of carbonyl groups (C6=O1...C12a=O2a) interact with the shortest O1...C12a distance (D1) of 3.319 Å and a narrow A1–A4 range of 79.4°–99.7°, as well as a small C=O...C=O torsion angle of 19.7°. The contact configuration differs remarkably from the sheared parallel motifs in **1** and **2**, but more close to the idealized antiparallel motif ($\tau = 0^\circ$; see Scheme 2) than the antiparallel motif (A1–A4 range of 54.8°–120.4°, $\tau = 57.0^\circ$ in **1** and 58.6° in **2**) observed in **1** and **2**. We designate it as an antiparallel motif, and the detailed metric geometries are shown in Table 2 for comparison. Notably, the C12=O2 group of the carbonyl...carbonyl interaction also approaches an adjacent 2,6-pyridinediyl ring with a distance from O2 to the ring centroid of 3.589 Å (Figure 4b), forming an unconventional C=O... π interaction, which is comparable with the C=O... π contact in pyridyl systems surveyed by us recently.¹⁵ The ...[C=O...C=O... π]_{*n*}... contact mode in the present case is shown and illustrated in Figure 4b.

In the complex [Ag(L)₂(PF₆)₂ (**4**), a centrosymmetric disilver(I) metallacyclophane [Ag₂(L)₂]²⁺ is formed by two μ_2 -bridging L ligands linking to two Ag(I) ions via their four 4-pyridyl rings (N1–Ag1 2.152(7) Å, N3–Ag1a 2.129(7) Å, N1–Ag1–N3a 174.4(2)°; a: $-x + 1, -y + 1, -z + 1$). Each Ag(I) ion also weakly links to four symmetry-related PF₆⁻ anions (P1 and P2 containing), exhibiting an octahedral N₂F₄-coordination geometry. The bulky and weakly coordinating PF₆⁻ anions are thus located around the metallacycle, as shown in Figure 5a. Along the *a* axis, PF₆⁻ anions (P1 containing) are sandwiched within the stacking metallacycles and link them through Ag...F interactions (Ag...F distance in the 2.973(6)–2.981(7) Å range)¹⁶ to form columns (Figure 5a). Along the *b* direction, the columns are interconnected by PF₆⁻ anions (P2 containing) arranged at the side of the [Ag₂(L)₂]²⁺ moieties through another set of Ag...F (3.173(6)–3.200(6) Å) interactions. Moreover, the columns interdigitate through outstretched pyridyl rings and interact via π ... π stacking between 4-pyridyl and 2,6-pyridinediyl rings with centroid...centroid separations ranging from 3.625 Å to 3.672 Å to generate a 3-D framework (Figure 5b). No carbonyl...carbonyl interaction is found in **4**, which may be attributed to the larger separation between the metallacycles by the bulky hexafluorophosphates.

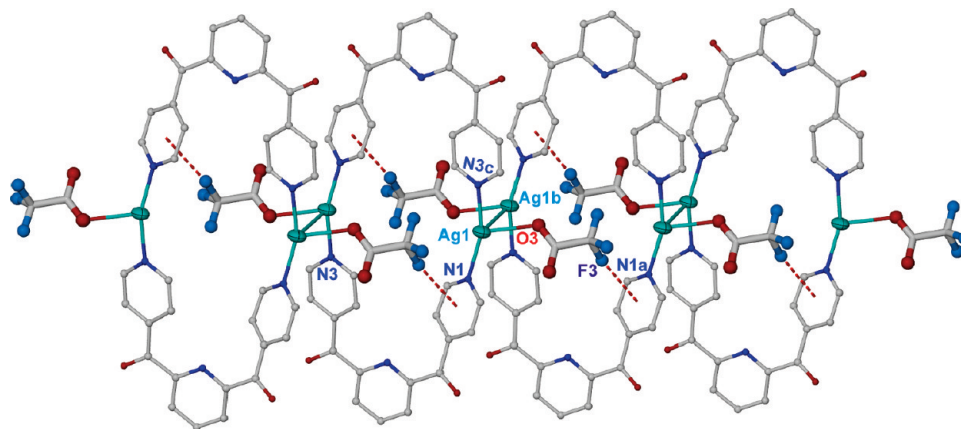


Figure 6. Anion- π (red dashed line) and argentophilic (turquoise bond) interactions between adjacent metallacycles in **5**. Symmetry codes: a: $x - 1, y, z$; b: $-x, -y + 1, -z + 1$; c: $-x + 1, -y + 1, -z + 1$.

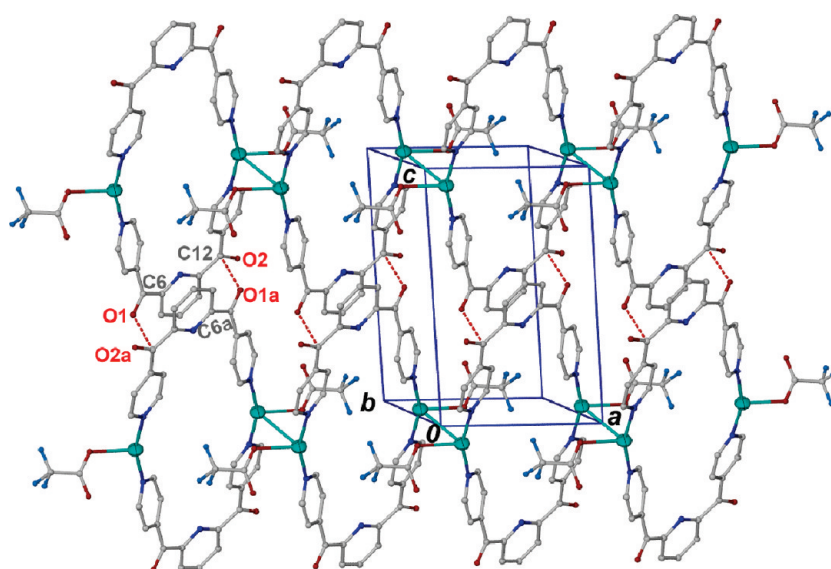


Figure 7. Carbonyl \cdots carbonyl interactions (red dashed lines) between chains in complex **5**. Symmetry code: a: $-x + 1, -y + 1, -z$.

$\{[Ag(L)(CO_2CF_3)]_2\}_\infty$ (**5**), $[Ag(L)]_2(SO_3CF_3)_2$ (**6**), and $[Ag(L)]_2(CO_2CF_2CF_3)_2$ (**7**) are isostructural complexes of **4** that show a common cationic $[Ag_2(L)_2]^{2+}$ metallacyclic skeleton and supramolecular aggregation with diverse counteranions. As for $\{[Ag(L)(CO_2CF_3)]_2\}_\infty$ (**5**), the counteranion (trifluoroacetate) links to the trigonally coordinated Ag(I) ion with Ag1–O3 bond length of 2.469(4) Å (Figure 6). As compared with **4**, the centrosymmetric metallacycles of **5** interconnect in a hand-in-hand mode through argentophilic (Ag1 \cdots Ag1b 3.036(9) Å) and anion- π interactions to generate an infinite chain along the *a* axis. As shown in Figure 6, the $CF_3CO_2^-$ anion approaches one pyridyl ring of an adjacent metallacycle with F3 \cdots N1a (the closest ring atom) distance of 3.276 Å and F3 \cdots centroid distance of 3.671 Å. Although a similar disilver(I) metallacyclic structure exists in **4** and **5**, the anion- π interactions drive the Ag(I) away from the normal linearly coordinated position, leading to a much smaller N1–Ag1–N3c angle of 158.77(2) $^\circ$ versus 174.4(2) $^\circ$ in **4**.

Careful scrutiny reveals that intermolecular carbonyl \cdots carbonyl interaction plays an important role in the supramolecular assembly of chains with $[Ag_2(L)_2]^{2+}$ metallacycles of **5**. As shown in Figure 7, the parallel chains are interlinked by

pairwise carbonyl \cdots carbonyl interactions between the rectangular $[Ag_2(L)_2]^{2+}$ motifs that are arranged in a head-to-tail mode. A layer in the *ac* plane is formed with the parallel chains bridged just by these interactions. Along the *b* axis, the stacking layers are further interconnected via C–H \cdots O=C hydrogen bonding¹⁷ ($R_2^2(10)$ motif, C10 \cdots O2a 3.350(6) Å, C10–H \cdots O2a 151 $^\circ$; a: $-x + 2, -y + 2, -z$) and O4–($CF_3CO_2^-$) \cdots C12b = O2b (O \cdots C = 3.360 Å; b: $x - 1, y - 1, z$) interactions,¹⁸ forming a 3-D supramolecular framework (Figure 8). In this case, the O1 \cdots C12a distance (D1) of 2.975 Å is shorter than those found in **1–3**. The A1 (C6=O1 \cdots C12a 125.6 $^\circ$; a: $-x + 1, -y + 1, -z$) and A2 (O1 \cdots C12a=O2a 102.6 $^\circ$) angles and torsion angle C6=O1 \cdots C12a=O2a of 110.4 $^\circ$ are similar to the sheared parallel motif manifested in **1** and **2** (see Table 1 and Figure 7).

The dinuclear $[Ag_2(L)_2]^{2+}$ moiety in $[Ag(L)]_2(SO_3CF_3)_2$ (**6**) exhibits a linearly coordinated silver(I) ion with a N1–Ag1–N3a bond angle of 172.88(1) $^\circ$, which is comparable with that of 174.4(2) $^\circ$ in the similar metallacycle of **4** (Figure 9). In the crystal structure of **6**, the $[Ag_2(L)_2]^{2+}$ metallacycles arranged in a shoulder-to-shoulder manner interact through pairs of intermolecular $\pi\cdots\pi$ interactions (centroid \cdots centroid distance 3.708 Å) between parallel

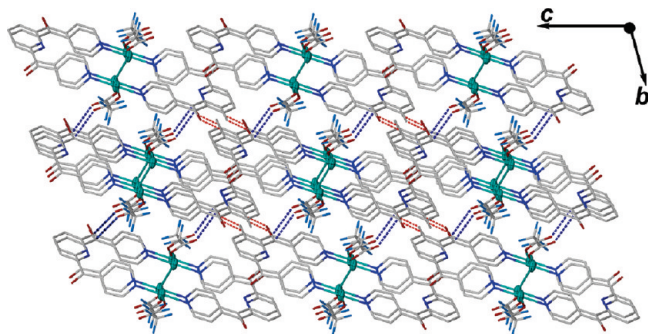


Figure 8. Interactions between layers in the ac plane of **5** viewed down the a axis; $C-H\cdots O=C$ ($R_2^2(10)$ motif, red dashed lines) hydrogen bonds and $O(CF_3CO_2^-)\cdots C=O$ (blue dashed lines). The carbonyl \cdots carbonyl interactions are omitted for clarity. All hydrogen atoms are also omitted except those involved in hydrogen bonding.

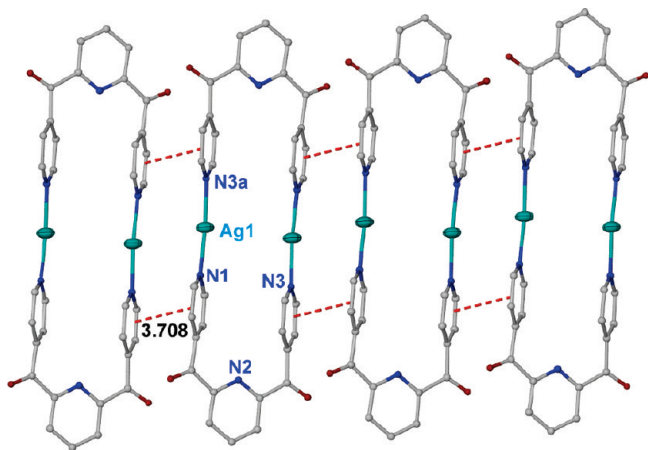


Figure 9. Infinite chain along the b direction in **6** constructed with linkage of $[Ag_2(L)_2]^{2+}$ metallacycles by $\pi\cdots\pi$ interactions between parallel 4-pyridyl rings. Symmetry code: $a: -x + 1, -y + 1, -z + 1$.

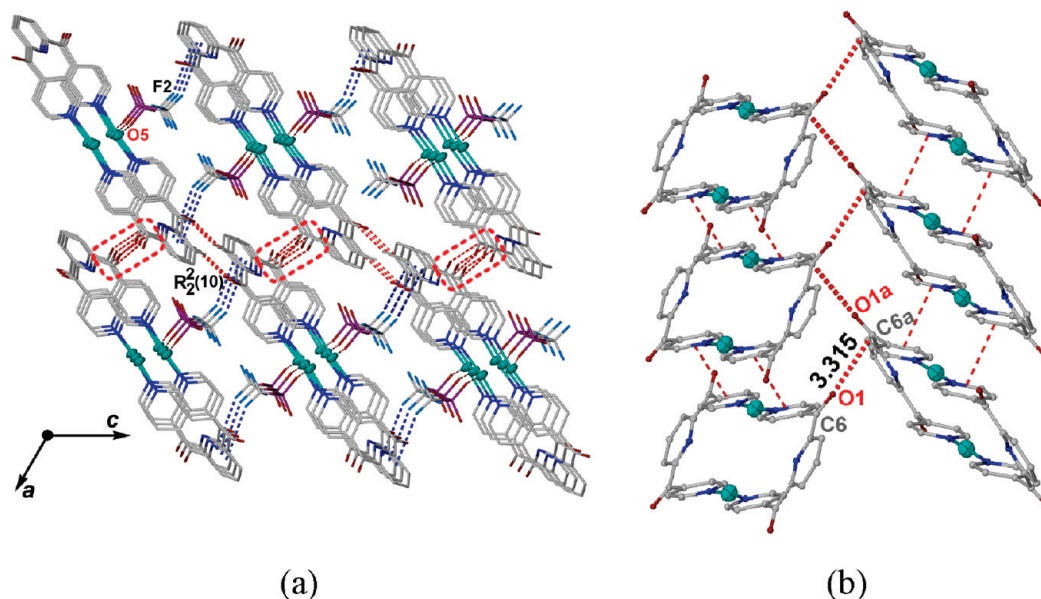


Figure 10. (a) Crystal structure of **6** viewed down the b direction, showing the supramolecular assembly with metallacyclic $[Ag_2(L)_2]^{2+}$ motifs via anion $\cdots\pi$ (blue dashed lines), carbonyl \cdots carbonyl contact (encircled portions, red dashed lines) and $C-H\cdots O=C$ hydrogen-bonding interactions ($R_2^2(10)$ motif, red dashed lines). Hydrogen atoms not participating in hydrogen bonding are omitted for clarity. The $\pi\cdots\pi$ interactions along the b axis are also omitted. (b) Carbonyl \cdots carbonyl interactions (thick dash lines) with the $\cdots[C=O\cdots C=O]_n\cdots$ array in the encircled portions of part (a). Symmetry code: $a: -x + 3/2, y + 1/2, -z + 3/2$.

4-pyridyl rings belonging to adjacent L ligands (Figure 9), forming a dense infinite chain in the b direction. The counterions occupy the interstices between the cationic $[Ag_2(L)_2]^{2+}$ chains, as opposed to the formation of a sandwich adduct in **4**. As shown in Figure 10a, along the c axis the triflate acts as a linker through weak $Ag\cdots O$ bonding ($Ag1\cdots O5$ 2.713(3) Å)¹⁹ to the dense cationic chain, and the $F(\text{triflate})\cdots\pi$ interaction [$F2\cdots$ centroid = 3.744 Å, $F2\cdots N2a$ (closest ring atom) is 3.293 Å; $a: x, -y + 1, z - 1/2$] bridges the 2,6-pyridinediyl ring of an adjacent chain, thus forming a layer in the bc plane. Along the a direction, the infinite chains are further connected by carbonyl \cdots carbonyl and $C10-H\cdots O2a = C12a$ ($a: -x + 3/2, -y + 1/2, -z + 2$) interactions ($R_2^2(10)$ motif, $C\cdots O$ 3.328(5) Å, $C-H\cdots O$ 139°), generating a 3-D framework (Figure 10a). As shown in Figure 10b, the contacted carbonyl groups are linked in a head-to-tail fashion with one O atom pointing to the other to bridge the adjacent chains together, yielding another infinite $\cdots[C=O\cdots C=O]_n\cdots$ array differing from that in **1** and **2** (Figure 2b). Atom O1 is in weak contact with C6a at an $O\cdots C$ distance (D1) of 3.315 Å. The $C6=O1\cdots C6a$ angle (A1) approaches 161.3° (close to 180°) and the $C6=O1\cdots C6a=O1a$ torsion angle is 72.1°, which differ much from the antiparallel motif and sheared parallel motif manifested in **1–3** and **5**, and accordingly we assign it to the perpendicular motif of Allen.^{3a} The detailed geometrical parameters are displayed in Table 2.

The dinuclear $[Ag_2(L)_2]^{2+}$ metallacycle in $[Ag(L)_2](CO_2CF_2CF_3)_2$ (**7**) is comparable to that in isostructural $\{[Ag(L)(CO_2CF_3)]_2\}_\infty$ (**5**) due to the alike nature of their counteranions. The $N1-Ag1-N3a$ angle of 144.95(2)° is similar to 158.77(2)° in **5**, but much smaller than 172.88(1)° in **6** and 174.4(2)° in **4**. As compared to **5**, the bulkier $CF_3CF_2CO_2^-$ exhibits a $\eta^1:\eta^2:\mu_2$ -bridging mode weakly bound to two Ag(I) ions from separate metallacycles with $Ag\cdots O$ distances lying within the 2.650(5)–2.750(4) Å range. Five-coordinate N_2O_3 -geometry of the Ag(I) ion involves two

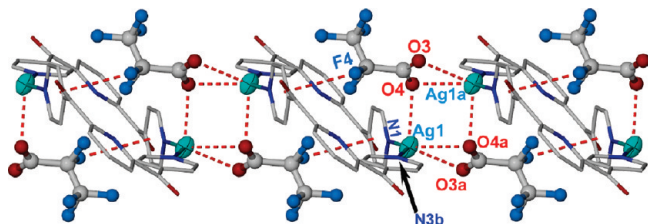


Figure 11. Ag \cdots O and anion- π interactions between [Ag $_2$ (L) $_2$] $^{2+}$ metallacycles in **7** arranged along the a axis; Ag1 \cdots O4 2.654(4) Å, Ag1 \cdots O4a 2.650(5) Å, Ag1 \cdots O3a 2.750(4) Å. Symmetry codes: a: $-x + 2, -y + 2, -z + 1$; b: $-x + 1, -y + 2, -z + 1$. All hydrogen atoms are omitted for clarity.

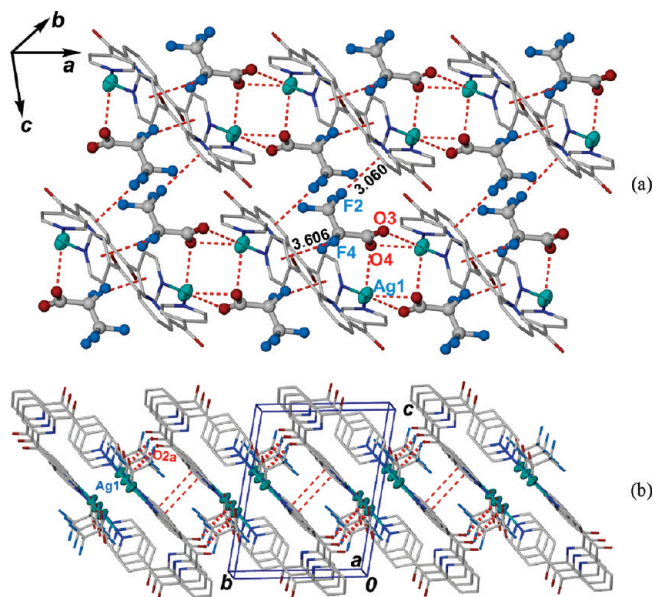


Figure 12. (a) Two-dimensional framework of **7** formed by linkage of [Ag $_2$ (L) $_2$] $^{2+}$ metallacycles via anion- π (F2 \cdots centroid 3.060 Å, F4 \cdots centroid 3.606 Å) and Ag \cdots O(anion) interactions. Ag \cdots O=C and $\pi\cdots\pi$ interactions are omitted for clarity. (b) Ag \cdots O=C (bold dashed lines) and $\pi\cdots\pi$ (thin dashed lines) connections in the formation of the 2-D framework viewed down the a axis. All anion- π and Ag \cdots O (anion) interactions are omitted for clarity. Symmetry code: a: $x + 1, y + 1, z$.

4-pyridyl N atoms and three O atoms of separate CF $_3$ CF $_2$ -CO $_2^-$, being different from the N $_2$ O-geometry in **5**. As shown in Figure 11, along the a axis the counteranion functions as a linker between adjacent [Ag $_2$ (L) $_2$] $^{2+}$ metallacycles through Ag \cdots O(C $_2$ F $_3$ CO $_2^-$) and F(anion) $\cdots\pi$ [F4 \cdots centroid 3.606 Å, F4 \cdots C(closest ring atom) 3.580 Å] interactions, forming an infinite chain. Along the b axis, one tail F2 atom of each CF $_3$ CF $_2$ CO $_2^-$ points to one central 2,6-pyridinediyl ring of an adjacent chain [F2 \cdots centroid distance 3.060 Å] (Figure 12a), another set of F $\cdots\pi$ contact, which combines with Ag \cdots O=C (Ag1 \cdots O2a 3.186 Å) and $\pi\cdots\pi$ (centroid \cdots centroid 3.925 Å, between 4-pyridyl rings) interactions to bridge the chains together to form a layer in the ab plane, as shown in Figure 12b. The multiple anion- π interaction of **7** involves contacts with two pyrazinyl rings (Figure 12a), which push the C $_2$ F $_3$ CO $_2^-$ away from the Ag(I) center, thus well accounting for the weak Ag \cdots O(C $_2$ F $_3$ CO $_2^-$) interaction in **7** as compared with the Ag-O(CF $_3$ CO $_2^-$) bonding in **5**. The F \cdots centroid(pyridyl) distances (3.060–3.671 Å) in **5** and **7** are slightly larger than those between s -tetrazine rings and the

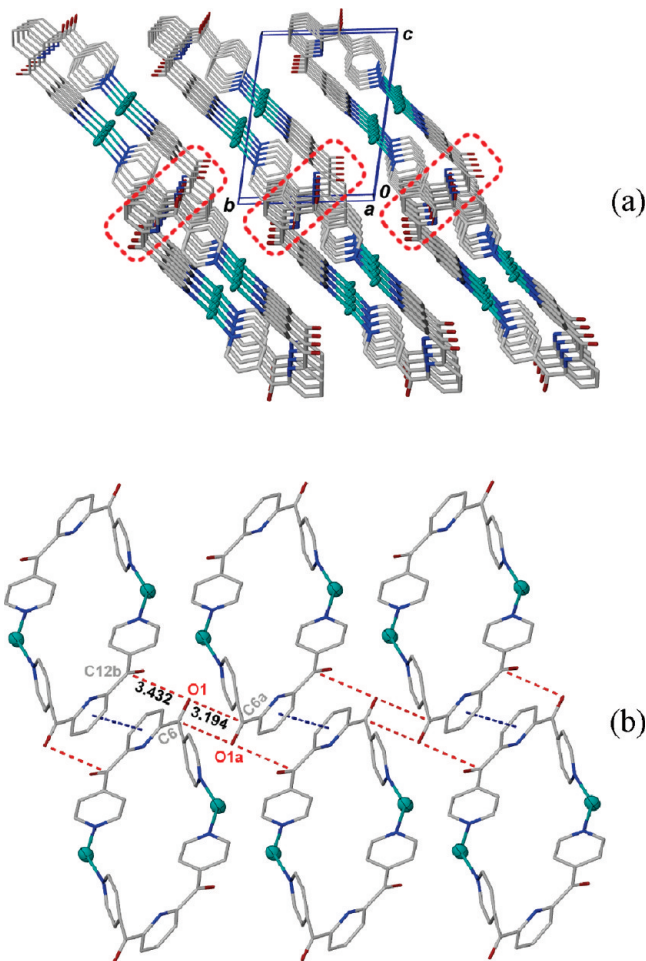


Figure 13. (a) Schematic showing the combined carbonyl \cdots carbonyl and $\pi\cdots\pi$ interactions that bridge the stacked [Ag $_2$ (L) $_2$] $^{2+}$ arrays along the a axis in **7**; the encircled portions indicate the sites of the cooperative interactions. Other interactions, all anions, and hydrogen atoms are omitted for clarity. (b) Details showing the carbonyl \cdots carbonyl and $\pi\cdots\pi$ interactions of an encircled portion in part (a). Symmetry codes: a: $-x + 1, -y + 1, -z$; b: $-x, -y + 1, -z$.

corresponding anions (2.840–3.265 Å) in silver(I) complexes 20 but compare well with those involving less π -acidic pyrazinyl and pyrimidinyl rings. 21

In the crystal structure of **7**, carbonyl \cdots carbonyl contact is found to cooperate with $\pi\cdots\pi$ stacking interaction between the 2,6-pyridinediyl rings (centroid \cdots centroid = 4.230 Å, closest ring atom to the centroid = 3.699 Å) to link the stacked layers parallel to the ab plane aforementioned (Figure 12b) together to form a three-dimensional supramolecular framework, as shown in Figure 13. Regarding the carbonyl \cdots carbonyl interaction in the present case, a pair of antiparallel carbonyl groups related by a C $_2$ axis at an O1 \cdots C6a distance (D1) of 3.194 Å (Figure 13) exhibit a typical idealized antiparallel motif (Table 2). Notably, the C6=O1 group also points toward another carbonyl (C12b=O2b) at one side of the extended antiparallel arrangement, resulting in a C=O \cdots C=O \cdots C=O contact manner with an O1 \cdots C12b (D1) distance of 3.432 Å. The torsion angle C6=O1 \cdots C12b=O2b is 117.8°, and $\Delta 1$ equals 88.0°, indicating a sheared parallel motif.

Role of Carbonyl \cdots Carbonyl Interaction. In the supramolecular conglomeration of silver(I) complexes **1–3** and

5–7, intermolecular carbonyl···carbonyl interaction is revealed as a common dominant noncovalent interaction that plays an important role. As structural analysis indicated that such weak noncovalent interaction rarely exists alone in small-molecule crystal structures based on CSD database research,²⁵ additional intermolecular interactions also coexist in complexes 1–3 and 5–7. In these complexes, the carbonyl···carbonyl interaction combines with Ag···Ag, π ··· π , hydrogen-bonding, Ag···O=C, O(anion)···C=O interactions, as well as unconventional C=O··· π and anion- π (pyridyl) interactions, to assemble different coordination motifs (infinite chains in 1–2, metallacycles in 3 and 5–7) into higher-dimensional supramolecular frameworks. The carbonyl···carbonyl interactions in 1–3 and 5–7 exhibit flexible contact configurations. The typical antiparallel motif occurs in 7 (A1–A4 = 90°, τ = 0°), the perpendicular motif is found in 6 (A1 close to 180°, τ = 72.1°), while the antiparallel and sheared parallel motifs in 1–3 and 5 have similar geometrical features (see Table 2). In the present context, we designate a carbonyl···carbonyl contact with a τ > 60° as sheared parallel and that with a τ < 60° as antiparallel motif. Furthermore, the antiparallel (in 1–3, 7) and sheared parallel (in 1–2, 5, and 7) motifs occur more frequently than the perpendicular motif (in 6) in the present series of silver(I) complexes, and the values of the A1 angle are commonly larger than those of other A2–A4 angles in each case. This result may be reasonably ascribed to the fact that when a pair of carbonyl groups comes into close contact, steric repulsion between substituents would lead to a larger A1 angle and preferred adoption of the antiparallel or sheared motifs rather than the perpendicular motif. This phenomena was observed in crystals of small organic molecules by Allen,³ and it also agrees well with a recent survey on the relative orientations of neighboring intermolecular carbonyls in organic crystals by Lee.⁴

Regarding the contact strength, in this study the measured values of D1 lie within a narrow 2.975–3.432 Å range, being comparable to the 2.92–3.32 Å range from ab initio calculations,^{3a} but slightly longer than 2.796 Å in the organometallic complex (η^5 -C₅H₅)W(CO)₃(η^5 -N-maleimidato) owing to the presence of the coordinated carbonyl group (ion-polarization) in the latter.⁹ Such intermolecular carbonyl···carbonyl interaction is a type of weak noncovalent interaction, which is competitive with hydrogen bond as already noted.^{3–5} The diversity of the presence and geometries of this type of intermolecular contact in complexes 1–7 well substantiates this conclusion. No carbonyl···carbonyl interaction is found in 4, while the contacts of 5–7 exhibit distinct configurations (sheared parallel motif in 5, perpendicular motif in 6 and typical antiparallel motif in 7) despite the fact that isostructural complexes 4–7 contain a similar dinuclear [Ag₂(L)₂]²⁺ metallacyclic skeleton. The present investigation shows that the nature of particular anions in isostructural complexes 4–7 has a subtle influence on the precise microarchitecture of these supramolecular aggregations, including the configurations of the weak carbonyl···carbonyl interaction.

Conclusions

In the present series of silver(I) complexes of 2,6-pyridinediylbis(4-pyridinyl)methanone ligand (L), complexes 1 and 2 are isomorphous helical polymers, and 3 is a metallacycle featuring a trisilver(I) core, while 4–7 are isostructural

complexes containing a common dinuclear [Ag₂(L)₂]²⁺ metallacyclic skeleton. Intermolecular multipolar carbonyl···carbonyl interaction is a common dominant interaction in complexes 1–3 and 5–7, which combine with argentophilic Ag(I)···Ag(I), heteroaromatic π ··· π , hydrogen-bonding, Ag···O=C, O(trifluoroacetate)···C=O, as well as unconventional C=O··· π and anion- π (pyridyl) interactions, to assemble the helical (1, 2) and metallacyclic moieties (3, 5–7) into higher-dimensional metal–organic frameworks. Three principal types of carbonyl···carbonyl interaction, namely, antiparallel, sheared parallel, and perpendicular motifs surveyed by Allen are substantiated and shown to play an important role in supramolecular conglomeration of these silver complexes. Unusual supramolecular associations such as “···[C=O···C=O]_n···” (in 1–2, 6) and “···[C=O···C=O··· π]_n···” (in 3) and “C=O···C=O···C=O” (in 7) are the novel structural features observed in this work. These dipolar···dipolar interactions exhibit variable geometrical arrangements in response to the presence of different coexisting counteranions, and their cooperative effect with other noncovalent interactions contrive to consolidate molecular packing in the crystal structures of 1–3 and 5–7.

Acknowledgment. This work is supported by the Hong Kong Research Grants Council (GRF Ref. No. CUHK 402206) and the Wei Lun Foundation.

Supporting Information Available: Crystallographic data of 1–7 in CIF format. This material is available free of charge via the Internet at <http://pubs.acs.org>. CCDC-789268–789274 contain the supplementary crystal data for 1–7, respectively. These data can be obtained free of charge from The Cambridge Crystallographic Data Centre via www.ccdc.cam.ac.uk/data_request/cif.

References

- (1) (a) Jeffrey, G. A.; Saenger, W. *Hydrogen Bonding in Biological Systems*; Springer-Verlag: Berlin, 1999; (b) Taylor, R.; Mullaley, A.; Müllier, G. W. *Pestic. Sci.* **1990**, *29*, 197–213.
- (2) Gavezzotti, A. *J. Phys. Chem.* **1990**, *94*, 4319–4325.
- (3) (a) Allen, F. H.; Baalham, C. A.; Lommerse, J. P. M.; Raithby, P. R. *Acta Crystallogr. B* **1998**, *54*, 320–329. (b) Deane, C. M.; Allen, F. H.; Taylor, R.; Blundell, T. L. *Protein Eng.* **1999**, *12*, 1025–1028. (c) Wood, P. A.; Borwick, S. J.; Watkin, D. J.; Motherwell, W. D. S.; Allen, F. H. *Acta Crystallogr. B* **2008**, *64*, 393–396. (d) Sparkes, H. A.; Raithby, P. R.; Clot, E.; Shield, G. P.; Chisholm, J. A.; Allen, F. H. *CrystEngComm* **2006**, *8*, 563–570.
- (4) Lee, S.; Mallik, A. B.; Fredrickson, D. C. *Cryst. Growth Des.* **2004**, *4*, 279–290.
- (5) (a) MacCallum, P. H.; Poet, R.; Milner-White, E. J. *J. Mol. Biol.* **1995**, *248*, 374–384. (b) Lario, P. I.; Vriellink, A. *J. Am. Chem. Soc.* **2003**, *125*, 12787–12794. (c) Pal, T. K.; Sankaramakrishnan, R. *J. Phys. Chem. B* **2010**, *114*, 1038–1049 and references therein.
- (6) (a) Berman, H. M.; Westbrook, J.; Feng, Z.; Gilliland, G.; Bhat, T. N.; Weissig, H.; Shindyalov, I. N.; Bourne, P. E. *Nucleic Acids Res.* **2000**, *28*, 235–242. (b) Allen, F. H. *Acta Crystallogr. B* **2002**, *58*, 380–388.
- (7) (a) Bürgi, H. B.; Dunitz, J. D.; Shefter, E. *J. Am. Chem. Soc.* **1973**, *95*, 5065–5067. (b) Bürgi, H. B.; Dunitz, J. D. *Acc. Chem. Res.* **1983**, *16*, 153–161. (c) Schweizer, W. B.; Procter, G.; Kafory, M.; Dunitz, J. D. *Helv. Chim. Acta* **1978**, *61*, 2783–2880.
- (8) Paulini, R.; Müller, K.; Diederich, F. *Angew. Chem., Int. Ed.* **2005**, *44*, 1788–1805 and references therein.
- (9) Palusiak, M.; Rudolf, B.; Zakrzewski, J.; Pfitzner, A.; Zabel, M.; Grabowski, S. *J. Organomet. Chem.* **2006**, *691*, 3232–3238.
- (10) SMART 5.0 and SAINT 4.0 for Windows NT, Area Detector Control and Integration Software; Bruker Analytical X-Ray Systems Inc.: Madison, WI, 1998.
- (11) Sheldrick, G. M. *SADABS: Program for Empirical Absorption Correction of Area Detector Data*; University of Göttingen: Göttingen, Germany, 1996.

- (12) Sheldrick, G. M. *SHELXTL 5.1 for Windows NT: Structure Determination Software Programs*; Bruker Analytical X-ray Systems, Inc.: Madison, WI, 1997.
- (13) Pauling, L. *The Nature of the Chemical Bond*; Cornell University Press: Ithaca, NY, 1960; p 260.
- (14) (a) Pyykkö, P. *Chem. Rev.* **1997**, *97*, 597–636. (b) Zhao, X.-L.; Wang, Q.-M.; Mak, T. C. W. *Inorg. Chem.* **2003**, *42*, 7872–7876 and references therein .
- (15) Wan, C.-Q.; Chen, X.-D.; Mak, T. C. W. *CrystEngComm* **2008**, *10*, 475–478.
- (16) Wang, Q.-M.; Mak, T. C. W. *Chem. Commun.* **2001**, 807–808.
- (17) Roesky, H. W.; Andruh, M. *Coord. Chem. Rev.* **2003**, *236*, 91–119.
- (18) (a) Chakrabarti, P.; Pal, D. *Protein Sci.* **1997**, *6*, 851–859. (b) Politzer, P.; Murray, J. S.; Clark, T. *Phys. Chem. Chem. Phys.* **2010**, *12* (28), 7748–7757.
- (19) Su, C.-Y.; Cai, Y.-P.; Chen, C.-L.; Smith, M. D.; Kaim, W.; zur Loye, H.-C. *J. Am. Chem. Soc.* **2003**, *125*, 8595–8613.
- (20) Schottel, B. L.; Bacsá, J.; Dunbar, K. R. *Chem. Commun.* **2005**, 46–47.
- (21) Black, C. A.; Hanton, L. R.; Spicer, M. D. *Inorg. Chem.* **2007**, *46*, 3669–3679.